To implant the device with a minimum of difficulties, the thickness of the device must be as thin as possible.

does not excite the retinal cells but does excite the PFM photosensor cells. We have confirmed that the firing rate increases as the input NIR light intensity increases. This demonstrates that the smart LSI-based stimulator activates the retinal cells through an input of NIR light and suggests that it could be applied to human retinal prosthesis. Figure 5(b) shows the dependence on the input NIR light intensity and clearly indicates that the firing rate increases in relation to the input light intensity. This in vitro experiment suggests the effectiveness of the PFM photosensor for a stimulator device in subretinal implantation.

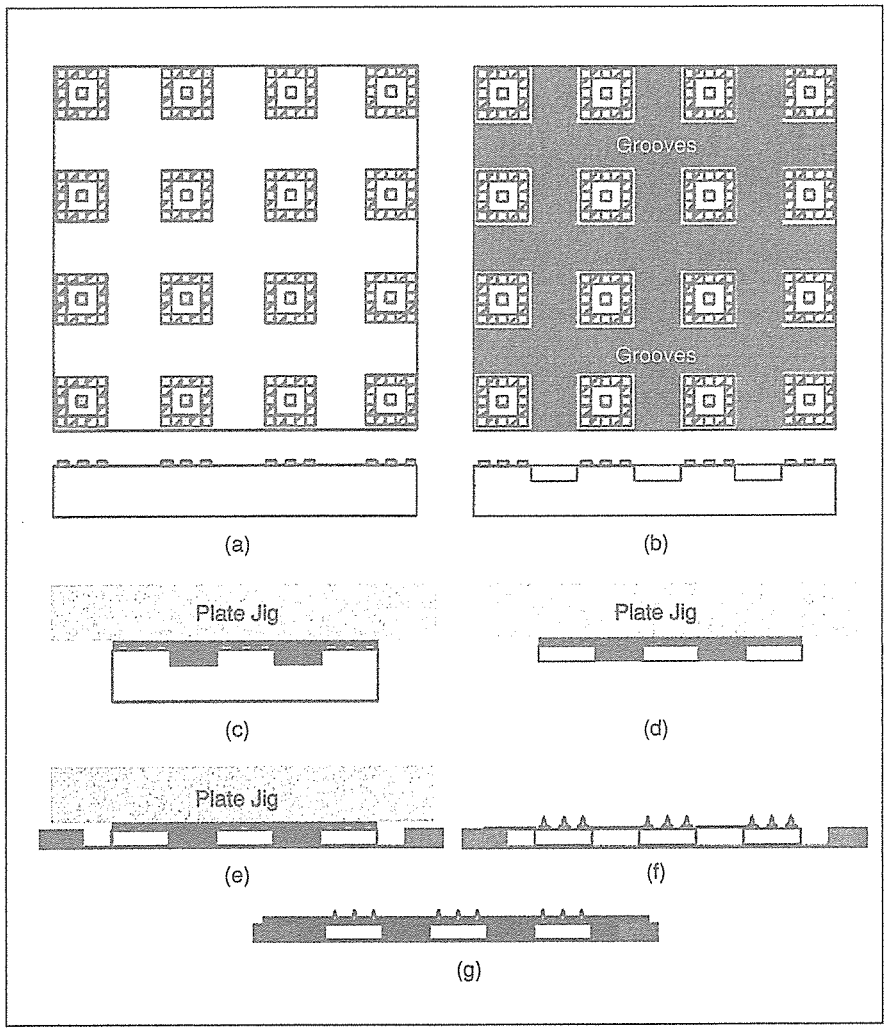

Fig. 7. The process flow of fabrication of the microchip-based stimulator (47). (a) bare die (4 × 4 microchips), (b) groove formation, (c) gluing wax onto a flat jig, (d) back-grinding and separation, (e) gluing onto a flexible substrate (thermal removal of jig), (f) wiring and bump forming, and (g) molding with epoxy resin.

The Microchip-Based Smart Stimulator

In the previous sections, we have demonstrated a smart LSI-based neural stimulator. To apply the device to a retinal prosthesis, however, it must be implanted in the eyeball and will inevitably be bent. As already mentioned, a thinned Si-LSI chip is fragile. Another issue arises associated with fragility; that is, how to realize a large number of electrodes using Si-LSI. For example, a 1,000-electrode array needs an area of over 10-mm^2, and the fragile characteristics of Si prevent such a large chip size. Thus, flexibility and extendibility are issues to be solved for the implementation of a Si-LSI stimulator as a retinal prosthesis device.

In this section, we propose and demonstrate a solution to the flexibility and extendibility limitations of our smart LSI-based stimulator. We have developed a new type of smart stimulator that consists of a number of microchips distributed on a flexible substrate. Figure 6 shows the concept and cross-sectional view of our smart distributed stimulator. The array consists of a number of LSI-based microchips, each of which is about 500-μm square. Each microchip has several Pt/Au stacked bump electrodes and is covered by the same process as described previously. We have developed two types of architecture for the microchip-based stimulator: broadcast and serial bus. The broadcast architecture is simple but only stimulates one electrode at a time, while the serial bus architecture consumes a large area for circuitry but stimulates multiple electrodes.

The Fabrication Process of Microchip-Based Smart Stimulator

For the smart distributed microchip architecture, we have developed a dedicated fabrication process. Figure 7 illustrates the process flow. The "mother" chip contains several of the microchips. In the mother chip, grooves over 100-μm deep are formed around the microchips by micromachining using an excimer laser. The chip is bonded upside-down to a plate jig with wax and is then thinned to a thickness

of 50–100 μm. Finally, the chip is bonded to a flexible polyimide substrate with thermosetting epoxy resin. The plate jig is automatically removed. The Pt/Au stacked bump electrodes and coating process are the same as previously described.

The fabricated stimulator is shown in Figure 8. To implant the device with a minimum of difficulties, the thickness of the device must be as thin as possible; our device has a thickness of around 200 μm, which is acceptable. As shown in Figure 8(b), the device can be bent easily. An image of the entire stimulator with platinum wires covered with silicone tubing is shown in Figure 8(c). The width of the stimulator is about 3 mm.

In order to validate the stimulator in semichronic implantation, we have fabricated a stimulator by the same process described above except, in this case, the microchip is just a silicon substrate with a single Pt/Au bump electrode formed on it. The stimulator was implanted in the sclera pocket of a rabbit, and the electrically evoked potential (EEP) with stimulating retinal cells was measured daily. After two weeks, the EEP signal slightly decreased but was measurable. These results demonstrate the possibility of applying the stimulator to retinal prostheses, although further studies are required to investigate long-term biocompatibility, safety, and other factors.

A Smart Distributed Stimulator with Broadcast Architecture

In the stimulator with broadcast architecture, the microchips are connected to each other via two wires (not including the power supply lines) and are placed on a flexible polyimide substrate. The features of the new chip are as follows. First, it is thin and bendable so that it can achieve closer contact with neural cells when implanted and, thus, is suitable for stimulating neural cells. Second, the incorporation of LSI in the microchip allows control and processing of the signals; for

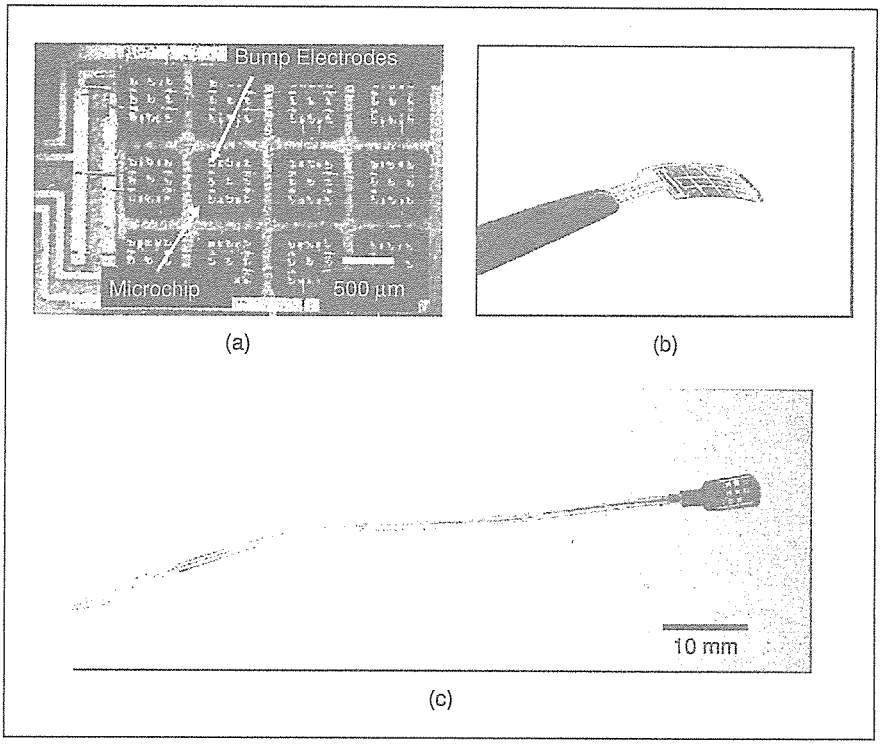

Fig. 8. Photographs of the fabricated microchip-based stimulator (47): (a) close-up of the microchips, (b) bending of the stimulator, and (c) the stimulator with platinum wires covered with silicone tubing.

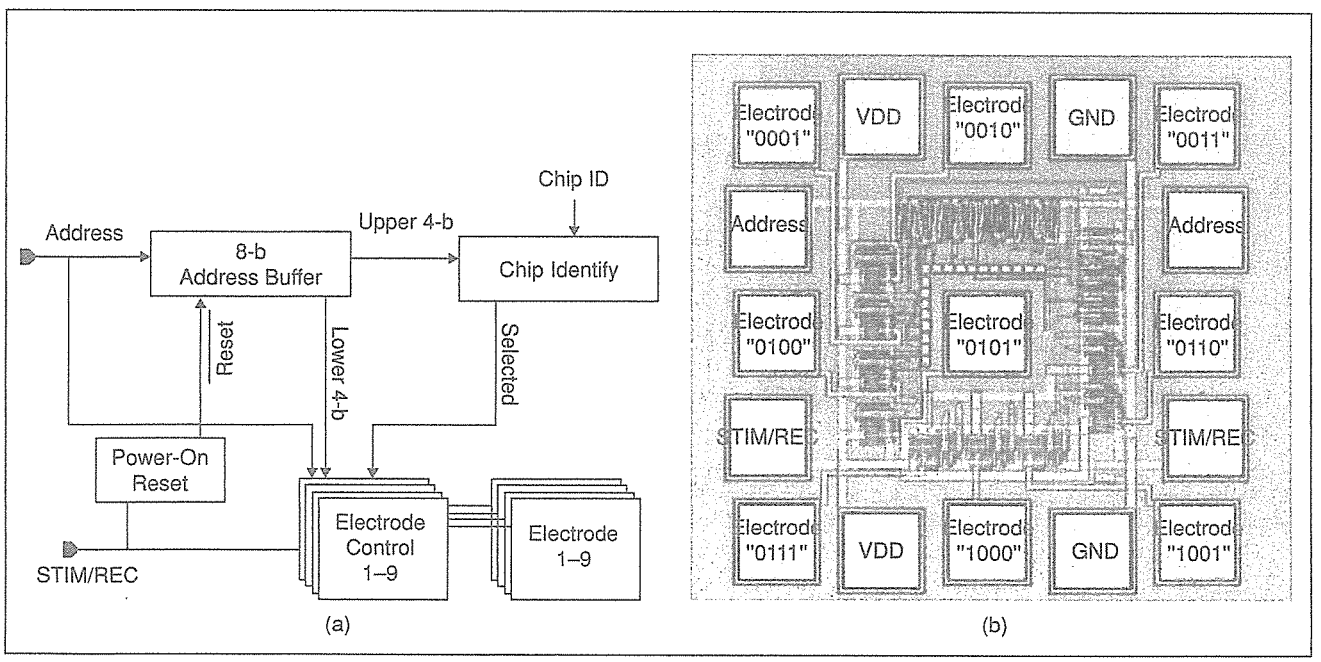

Fig. 9. (a) The circuit diagram and (b) layout of the microchip with broadcast architecture (48).

The application of LSI technologies confers benefits such as versatility, signal integrity, and compactness.

example, on-chip amplification circuitry enhances the signal-to-noise ratio in the monitoring of the electrode impedance, and both sensing and detecting can be implemented on the same chip. This provides the device with high performance and versatility. In addition, LSI reduces the input/output pads needed in the device such that only two signal lines for stimulation/record and control are required apart from the power supply lines. The control line operates the entire set of microchips, and each microchip includes enough circuitry to decode the control signal. Third, the device can be connected with another device; such a "daisy chain" could combine a large number of electrodes, for example, over 1,000 electrodes.

Figure 9 shows the circuit block diagram and the layout of the microchip [44], [45]. The chip is fabricated using 0.6-μm 2-poly 3-metal standard CMOS technology. The microchip is so small, at 600 μm $\times$ 600 μm, that it can be thinned down to less than 100 μm without risk of it breaking, as shown in Figure 8(b). The fabricated microchip has nine stimulation/recording electrodes and control circuits with four input/output (I/O) pads for addressing (ADDRESS) and stimulation/recording (STIM/REC) and four pads for power supply (VDD and GND), as shown in Figure 10. It is to be noted that each microchip relays ADDRESS and STIM/REC lines in the vertical direction and VDD and GND lines in the horizontal direction (Figure 10). This wiring architecture reduces the wiring area on the substrate.

We use a broadcast topology to assign one electrode to be activated; this consumes only a small area of circuitry, sufficiently small for the size of the microchip. An external controller broadcasts a control signal to all of the microchips. Each microchip has its own identification tag (ID). The microchip has an 8-b asynchronous counter as an address buffer [see Figure 9(a)]. The addressing counter counts the digital pulses applied to the ADDRESS line, and the microchip interprets the value in the counter as the address of the selected electrode. The upper 4 b and the lower 4 b represent the addresses of the selected chip and the selected electrode, respectively. Only the selected electrode on the selected chip is connected to the STIM/REC line. Once selected, neural stimulation/recording can be activated at the selected electrode via the STIM/REC line. The ID of each microchip is shown in Figure 10(a). Figure 10(b) shows experimental results of the fabricated stimulator in a saline solution. In each timing, only one electrode is activated, thus demonstrating that an arbitrary electrode can be selectively activated.

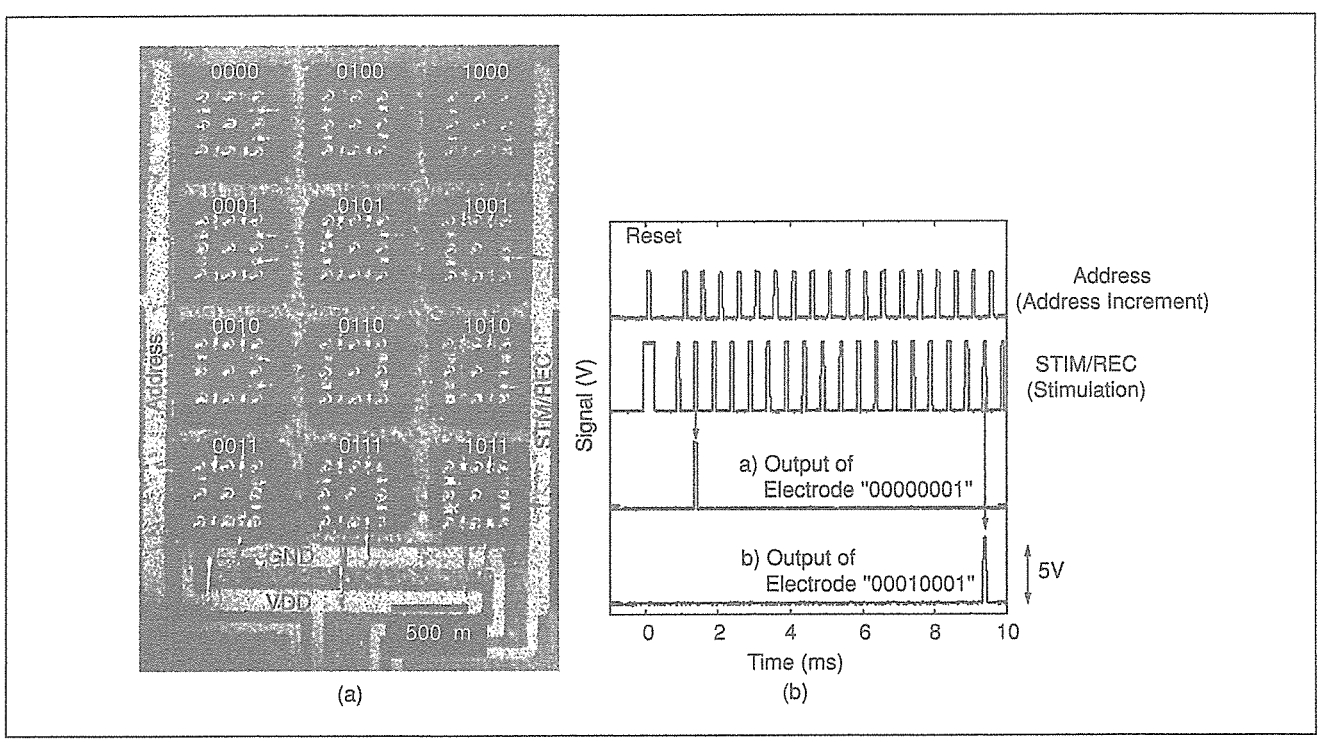

Fig. 10. (a) Connection diagrams of a 4 $\times$ 4 microchip-based stimulator and (b) the output waveforms from the stimulator in saline solution (47). The four-digit numbers are the microchip IDs.

Introducing the serial bus architecture enables the stimulator to vary in pulse parameters such as amplitude and duration for each microchip through the serial interface.

It should be noted that the number of microchips to be controlled is restricted by the asynchronous counter design and that the number could easily be increased if we design the counter with longer bits. Figure 11 illustrates the extendibility of the fabricated device: two stimulators consisting of 4 × 4 microchips with nine electrodes on each microchip (total 144 electrodes) are connected; thus, a stimulator with 288 electrodes is realized.

The Microchip-Based Neural Interface Device with Serial Bus Architecture

The broadcast architecture described in the previous section is simple but cannot realize independent control of the stimulus parameters for each microchip. In this section, we describe the next-generation microchip-based device, which integrates a single-wire serial interface, a PFM-based photosensor, an image processing circuit, and a current driver circuit [43]. Introducing the serial bus architecture enables the stimulator to vary in pulse parameters such as amplitude and duration for each microchip through the serial interface. The microchip is fabricated by 0.6-μm CMOS technology and is 500 μm × 500 μm. A microphotograph of one of the microchips is shown in Figure 12(a).

Special care is taken in the design in consideration of power consumption because we assume stimulator operation of a number of the microchips via wireless communication, which

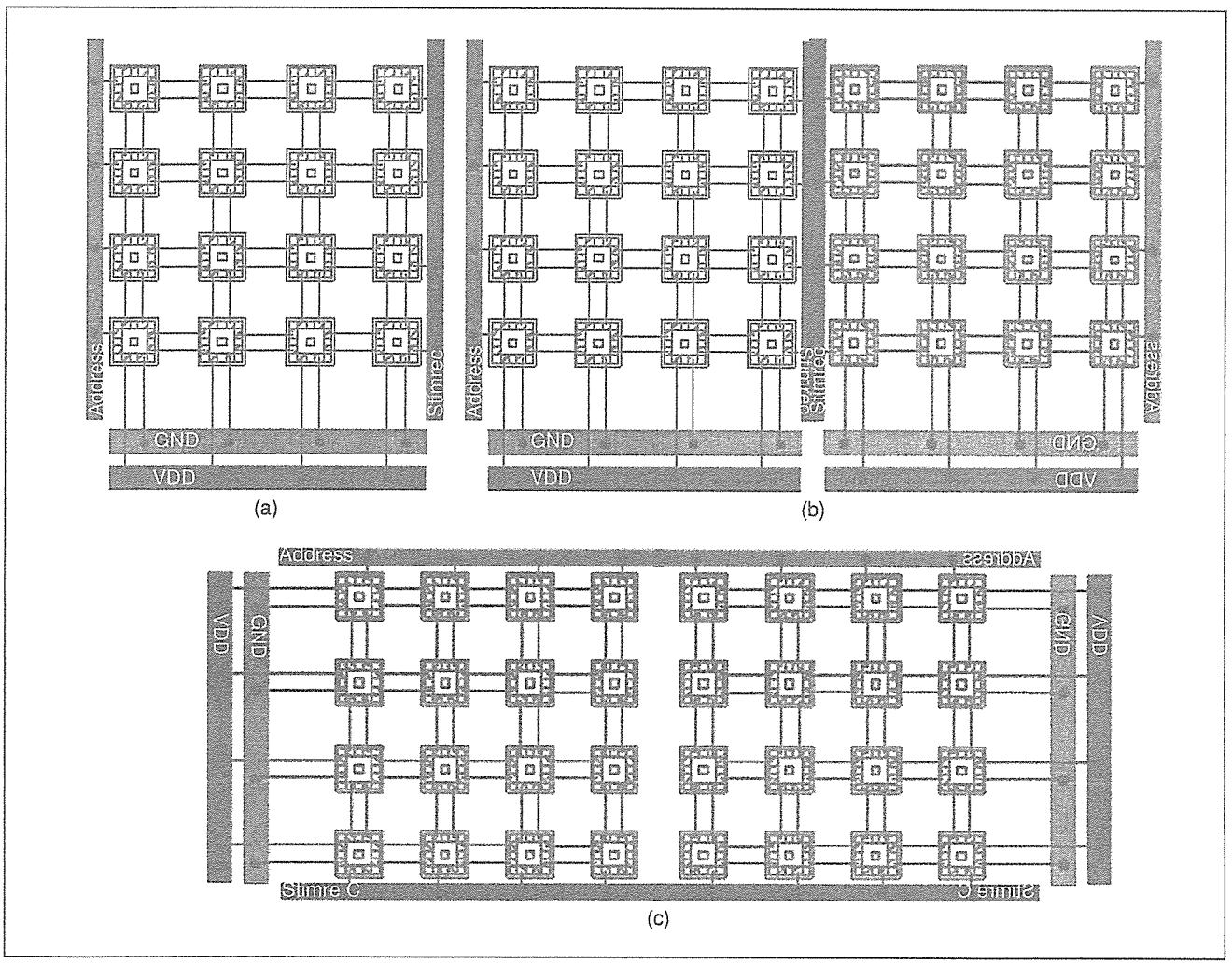

Fig. 11. Extendibility of the proposed stimulator: (a) original stimulator, (b) two stimulators with horizontal connection, and (c) two stimulators with vertical connection.

We intend to design a microchip with a simpler serial bus architecture that includes Pt/Au stacked bump electrodes.

limits the usable power of the device. The operation is described in detail in [43] and is briefly mentioned here. The data transaction is based on packets as shown in Figure 12(b). The packet is transmitted on a serial bus line, which is a physical connection between the microchips. A packet consists of an 8-b address bit field followed by an 8-b data bit field. The address assigns one of 254 microchips, and the data sets the stimulus amplitude parameters. After receiving two packets, the microchip is activated for photodetection and outputs stimulus currents; the pulse duration is the same as that of the clock as shown in Figure 12(b). Figure 12(c) shows experimental results of operation for three microchips, denoted as

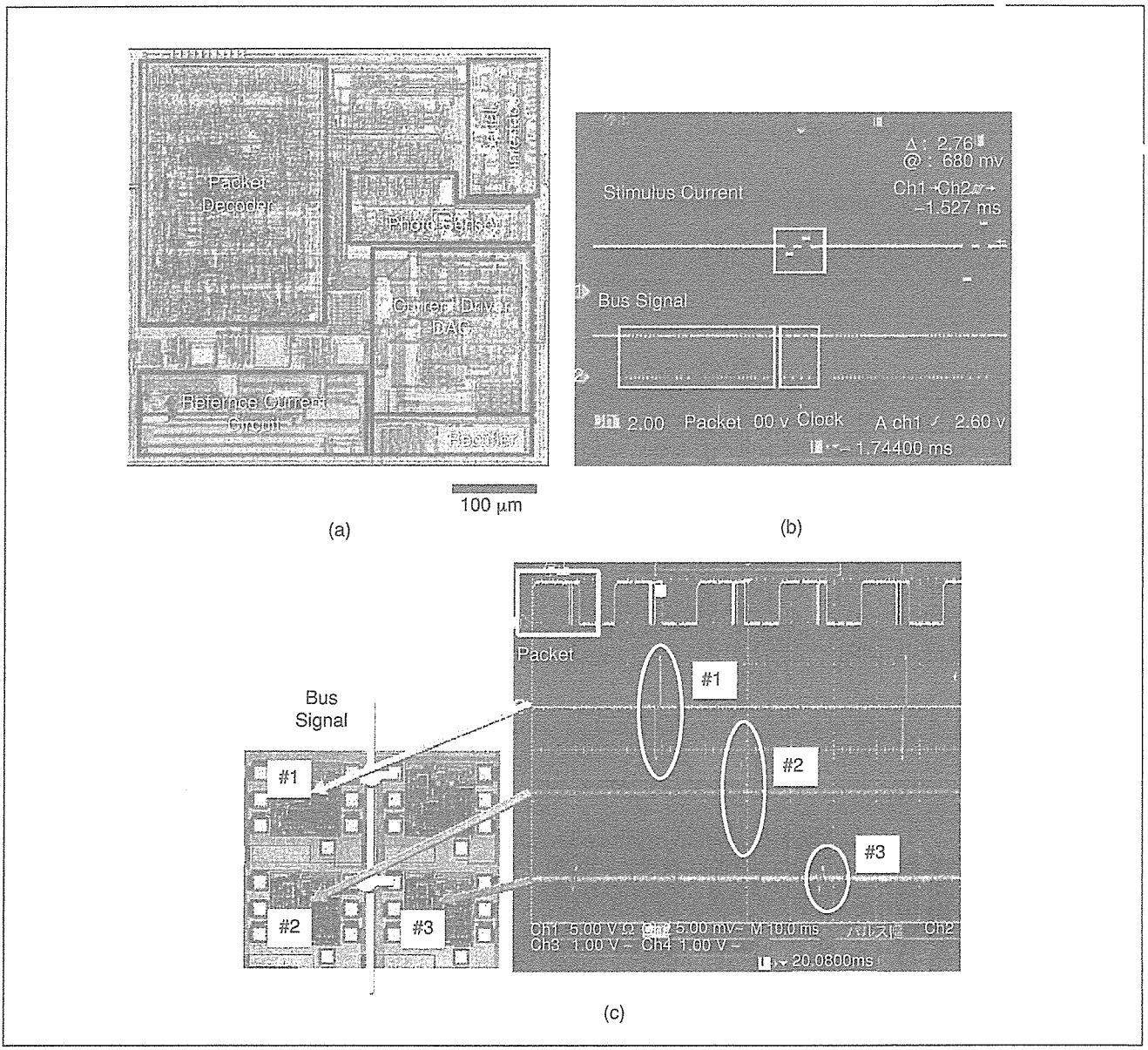

Fig. 12. Microchip-based stimulator with serial bus architecture (46). (a) Microphotograph of the fabricated microchip. Experimental results of (b) oscilloscope waveforms of the bus signal and the stimulus signal. (c) Oscilloscope waveforms of packet and the stimulus signals for #1, #2, and #3 microchips. The corresponding positions of the microchips are shown.

#1, #2, and #3. According to the bus signals, the three microchips produce different output current pulses.

The present microchip design mainly focuses on circuit architecture, and thus the device is not integrated with any electrodes. In the next step, we intend to design a microchip with a simpler serial bus architecture that includes Pt/Au stacked bump electrodes.

Conclusions

We have developed Si-LSI-based smart neural stimulators for retinal prosthesis. The application of LSI technologies confers benefits such as versatility, signal integrity, and compactness but requires a dedicated process for the integration and packaging of electrodes with the standard LSI structure. For this purpose, we have developed a Pt/Au stacked bump electrode stimulator with epoxy molding, which is suitable for forming on standard LSI chips and is effective in stimulating retinal cells. This stimulator has been evaluated in saline solution and in an in vivo experiment using detached frog retina. The positive results obtained suggest its potential in retinal prosthesis.

In summary, we have demonstrated a flexible and extendable microchip-based stimulator in which a number of microchips are distributed on a flexible polyimide substrate. Two types of such a microchip-based stimulator have been prepared: a broadcast type and a serial bus type. Both types demonstrate fundamental operations and show promising capability. In the next stage, we are planning to implant our developed microchip-based stimulator in animals to further confirm the possibility of application to human retinal prosthesis.

Acknowledgments

The authors would like to thank Prof. Tetsuya Yagi of Osaka University for the valuable discussion of in vitro experiments, Kazuaki Nakauchi of Osaka University for the semichronic data of the implanted stimulator, and Hiroyuki Tashiro of Kyushu University, Kenzo Shodo and Hiroyuki Kanda of Vision Institute, Nidek Co. Ltd. for the valuable discussion of electrodes. They also wish to thank Dr. Shigeru Nishimura and Naoko Tsunematsu of Tokyo Research Center, Nidek Co. Ltd. for their continuous encouragement and valuable discussion. This work was partly supported by the New Energy Development Organization (NEDO) of Japan ("Artificial Vision System," Prof. Y. Tano, project leader), and by Health and Labor Sciences Research Grants, Japan (Prof. Y. Tano, principal investigator).

Jun Ohta received the B.E., M.E., and Dr. Eng. degrees in applied physics, all from the University of Tokyo, Japan, in 1981, 1983, and 1992, respectively. In 1983, he joined Mitsubishi Electric Corporation, Hyogo, Japan, where he has been engaged in the research on optoelectronic integrated circuits, optical neural networks, and artificial retina chips. From 1992–1993, he was a visiting researcher in Optoelectronics Computing Systems Center, University of Colorado at Boulder. In 1998, he has been an associate professor at Graduate School of Materials Science, Nara Institute of Science and Technology (NAIST), Nara, Japan, and in 2004, he has been the professor of NAIST. His current research interests include vision chips, complementary metal oxide semiconductor image sensors, retinal prosthesis devices, biophotoniclarge-scale-integrations (LSIs), and integrated photonic devices.

He received the Best Paper Award of the Institute of Electronics, Information, and Communication Engineers IEICE Japan in 1992, the Ichimura Award in 1996, and the National Commendation for Invention in 2001. He is a member of the Japan Society of Applied Physics, the Institute of Electronics, Information and Communication Engineers of Japan, the Institute of Image Information and Television Engineers of Japan, Japanese Society for Medical and Biological Engineering, the Institute of Electronic and Electronics Engineers, and the Optical Society of America.

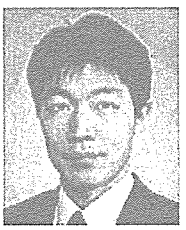

Takashi Tokuda received his B.S. and M.S. degrees in electronic engineering from Kyoto University, Kyoto, Japan, in 1993 and 1995, respectively. He received his Dr. Eng. degree in materials engineering from Kyoto University in 1998. He has been an assistant professor in the Graduate School of Materials Science, Nara Institute of Science and Technology, since 1999.

He has been working on photonic materials science and photonic device engineering. His research interests include CMOS image sensors, retinal prosthesis devices, bioimaging sensors, and biosensing devices. He is a member of the Japan Society of Applied Physics, and the Institute of Electronics, Information and Communication Engineers of Japan.

Keiichiro Kagawa received his B.E. degree in applied physics from Osaka University, Japan, in 1996. He received his M.E. and Dr. Eng. degrees in material and life science in 1998 and 2001, respectively. From 1995–2001, he was engaged in research on optical packaging and prototyping of optoelectronic parallel computers. Since 2001, he has been an assistant professor at the Nara Institute of Science and Technology, Nara, Japan.

His research interests include complementary metal oxide semiconductor image sensors, vision chips, and optoelectronic systems. He is a member of the Japan Society of Applied Physics, the Institute of Image Information and Television Engineers of Japan, and the IEEE.

Tetsuo Furumiya received the B.S. degree in mechanical engineering from Kansai University, Osaka, Japan, and the M.S. degree from Nara Institute of Science and Technology, Nara, Japan, in 2001 and 2003, respectively. Currently, he is working toward the Ph.D. degree at Nara Institute of Science and Technology.

Akihiro Uehara received the B.S. degree in electrical engineering from Osaka University, Japan in 1997. He received M.S. and Dr. Eng degrees from Nara Institute of Science and Technology, Nara, Japan, in 2000 and 2005, respectively.

In 2002, he joined the Nidek Vision Institute, Nidek Co., Ltd., Japan, where he has been engaged in the research of artificial vision prosthetic devices. His research interest is in complementary metal oxide semiconductor sensors and mixed-signal circuit design.

Yasuo Terasawa received the B.S. degree in applied physics from Tohoku University, Japan, in 1996, and an M.S. degree in information science from Tohoku University, Japan, in 1998. He joined Nidek Co., Ltd., Japan in 2001, working on the development of the retinal prosthesis. His research includes electrode technology, implantable electrical systems, and psychophysical evaluation of the prosthetic vision.

Motoki Ozawa received the B.E. degree in chemical engineering from Nagoya University, Japan, in 1985. He received M.S. degree in optics from the University of Rochester, New York, in 1987.

In 1988, he joined Dai Nippon Printing Co., Ltd., Japan, where he participated in commercialization of a digital proof printer and an electrical publishing system. In 1992, he joined Nidek Co., Ltd., Japan, where he worked on the research and development (R&D) of an excimer laser corneal surgery system. In 2003, he has been a director of the R&D division of Nidek, and since 2005, he has been a vice president of Nidek.

Takashi Fujikado is a professor of applied visual science at Osaka University Medical School, Japan. He received the B.S. and M.E. degrees from Tokyo University, Tokyo, Japan, in 1976 and 1978, respectively. He received the M.D. and Ph.D. degrees from Osaka University in 1982 and 1989, respectively.

Since joining in the department of Ophthalmology, Osaka University Medical School in 1985, he has been engaged in the research and clinical works on pediatric ophthalmology and neuro-ophthalmology. Currently, he is a member of Japanese Consortium for Artificial Retina and is engaged in the functional assessment of artificial retina.

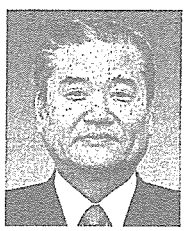

Yasuo Tano is the professor and chairman of the Department of Ophthalmology at Osaka University Medical School as well as the vice president of the Osaka University Hospital, Japan. He is the president of the Japanese Ophthalmological Society that holds more than 13,000 members. He is currently the president of Asia-Pacific Academy of Ophthalmology, which covers an area with more than half of world population. He is the executive editor of the Japanese Journal of Ophthalmology and is a member of many international editorial boards of prominent peer-review journals. He is also a member of the International Council of Ophthalmology, the Advisory Committee for the International Council of Ophthalmology, the Academia Ophthalmologica Internationalis (Chair V) and the Executive Committee for the Club Jules Gonin and is a charter member of the International Council of Ophthalmology Foundation.

He received his M.D. from Osaka University Medical School in 1972. After completing his residency in Japan, he became a vitreoretinal research fellow at Bascom Palmer Eye Institute, Miami, Florida, in 1977 and then at Duke Eye Center, Durham, North Carolina, in 1978. Tano has authored and coauthored over 550 English and Japanese publications in various fields of ophthalmology and has written or edited over 50 books and chapters on related topics. Tano has delivered many important lectures both domestically and internationally, including the Sir Norman McAllister Gregg Lecture at the 2000 Annual Meeting of the Royal Australian and New Zealand College of Ophthalmologists, the Pyron Lecture at the 19th Annual Meeting of the Vitreous Society, and the LIX Jackson Memorial Lecture.

Tano was one of the first to perform vitrectomy in Japan and has since dedicated his time in training aspiring surgeons in the field of vitreoretinal surgery. He is the pioneer in non-vitrectomised macular surgery and is one of the leading surgeons in macular translocation. He has invented many vitreoretinal instruments, which have contributed to advances in vitreoretinal surgery in the last decade.

Address for Correspondence: Jun Ohta, Graduate School of Materials Science, Nara Institute of Science and Technology, Takayama 8916-5, Ikoma, Nara 630-0101 Japan. E-mail: ohta@ms.naist.jp.

References

[1] M.A.L. Nicolelis, Ed. *Methods for Neural Ensemble Recordings*. Boca Raton, FLA: CRC Press, 1999.

[2] J. Chen, K.D. Wise, J.F. Hetke, and S.C. Bledsoe Jr., "A multichannel neural probe for selective chemical delivery at the cellular level," *IEEE Trans. Biomed. Eng.*, vol. 44, no. 8, pp. 760–769, 1997.

[3] Q. Bai, K.D. Wise, and D.J. Anderson, "A high-yield microassembly structure for three-dimensional microelectrode arrays," *IEEE Trans. Biomed. Eng.*, vol. 47, no. 3, pp. 281–289, 2000.

[4] M.O. Heuschkel, M. Fejtl, M. Raggenbass, D. Bertrand, and P. Renaud, "A three-dimensional multi-electrode array for multi-site stimulation and recording in acute brain slices," *J. Neurosci. Methods*, vol. 114, no. 2, pp. 135–148, 2002.

[5] T. Kawano, Y. Kato, M. Futagawa, H. Takao, K. Sawada, and M. Ishida, "Fabrication and properties of ultrasmall Si wire arrays with circuits by vapor-liquid-solid growth," *Sens. Actuators A, Phys.* vol. 97–98, pp. 709–715, 2002.

[6] E. Margalit, J.D. Weiland, R.E. Clatterbuck, G.Y. Fujii, M. Maia, M. Tameesh, G. Torres, S.A. D'Anna, S. Desai, D.V. Piyathaisere, A. Olivi, E. de Juan, and M.S. Humayun, "Visual and electrical evoked response recorded from subretinal electrodes implanted above the visual cortex in normal dogs under two methods of anesthesia," *J. Neurosci. Methods*, vol. 123, no. 2, pp. 129–137, 2003.

[7] S. Takeuchi, T. Suzuki, K. Mabuchi, and H. Fujita, "3D flexible multichannel neural probe array," *J. Micromech. Microeng.*, vol. 14, no. 1, pp. 104–108, 2004.

[8] T. Suzuki, D. Ziegler, K. Mabuchi, and S. Takeuchi, "Flexible neural probes with micro-fluidic channels for stable interface with the nervous system," in *Proc. 26th Int. Conf. IEEE EMBS*, San Francisco, California, 1–5 Sept. 2004.

[9] L. Johnson, F.K. Perkins, T. O'Hearn, P. Skeath, C. Merritt, J. Frieble, S. Sadda, M. Humayun, and D. Scribner, "Electrical stimulation of isolated retinal with microwire glass electrodes," *J. Neurosci., Methods*, vol. 137, no. 2, pp. 265–273, 2004.

[10] R. Rathnasingham, D.R. Kipke, S.C. Bledsoe Jr., and J.D. McLaren, "Characterization of implantable microfabricated fluid delivery devices," *IEEE Trans. Biomed. Eng.*, vol. 51, no. 1, pp. 138–145, 2004.

[11] R.J. Vetter, J.C. Williams, J.F. Hetke, E.A. Nunamaker, and D.R. Kipke, "Chronic neural recording using silicon-substrate microelectrode arrays implanted in cerebral cortex," *IEEE Trans. Biomed. Eng.*, vol. 51, no 6, pp. 896–904, 2004.

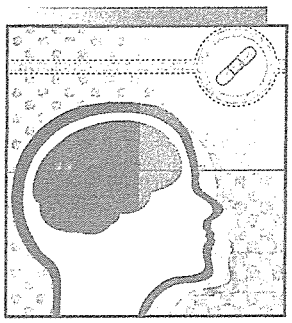

©EYEWIRE

Intraocular Retinal Prosthesis

Big Steps to Sight Restoration

BY JAMES D. WEILAND
AND MARK S. HUMAYUN

Retinal prostheses have the potential to restore some level of visual function to blind individuals. While visual prosthetic devices for the optic nerve and visual cortex also have potential application, the retinal approach offers the advantage of relatively accessible retinal neurons in the back of the eye. Biological studies have demonstrated biocompatibility of implantation and stimulation and have investigated retinal response to stimulation. Recent clinical trials have shown that a prototype epiretinal implant, despite having few electrodes contacting the retina, still allows test subjects to perform simple visual tasks. Ongoing engineering research is focusing on the fabrication of a high-resolution implant.

Introduction

Electrical stimulation to restore lost senses and modulate dysfunctional neural systems has gained increasing acceptance by clinicians [1], [2]. The cochlear implant is the most successful neural prosthesis. Deaf individuals can understand speech even though the cochlea is stimulated only at a few locations. A deep-brain stimulator to combat Parkinsonian tremor has recently been approved by the U.S. Food and Drug Administration. Yet, restoration of the sense of vision has not been possible. It has been known since the late 1960s that blind humans can perceive electrically elicited phosphenes in response to either retinal or cortical stimulation [3]. It took until the early 1990s for the fields of microfabrication and retinal surgery to advance to the point where it made sense to begin development of an implantable prototype retinal stimulator. Since then, a retinal prosthesis to restore vision to the blind has progressed rapidly from the conceptual phase to prototype medical devices undergoing clinical trials. Figure 1 shows a conceptual drawing of a retinal prosthesis.

The retina lines the back of the vitreous cavity, a 6 cm^3 fluid-filled space in the back of the eye that is normally filled with vitreous gel (Figure 2). The diseases that potentially can be treated by a retinal prosthesis are outer-retinal diseases, which include age-related macular degeneration and retinitis pigmentosa. These maladies are presently incurable and afflict hundreds of thousands worldwide [4], [5]. They primarily affect the photoreceptors of the retina, leaving the other retina layers relatively spared [6]. However, the other retinal cells are modified after photoreceptor loss [7]. The degree of modification is related to the time after photoreceptor loss. The dendritic trees of the bipolar and ganglion cells retract, and cells migrate into different layers. A thick glial seal forms between the retina and the subretinal space (where the photoreceptors used to be). In other words, after degeneration of the photoreceptors, the remaining retina also undergoes significant change.

Although the idea of replacing a lost sense of vision with an electronic device can be traced to a patent awarded to Graham Tassicker [8], the realization of a device suitable for initial testing in humans required years of advances in vision science, retinal surgery, and microelectronics. Many more technical advances will be needed to implement a high-resolution implant. However, the research that has been accomplished to date provides strong evidence that a high-resolution device may restore significant vision. Testing of prototype low-resolution devices has demonstrated that totally blind individuals can discriminate simple objects [9], [10]. This review will summarize the important findings to date from preclinical biological testing and clinical trials of retinal stimulation as well as briefly discuss recent technical advances. For lengthier reviews of retina implants, the reader is referred to recent publications [11], [12].

Other Approaches to Artificial Vision

Experimental artificial vision systems have electrically stimulated other anatomical locations in the visual system. The first experimental work towards a visual prosthesis began with electrical stimulation of the visual cortex using a grid of large surface electrodes. This has progressed to microelectrode arrays that penetrate deep into the cortex. A brief summary of the important findings in visual cortex stimulation is given below.

The seminal experiment in this field (and possibly in the field of neural prosthesis) was performed by Giles Brindley in 1968 [13]. Brindley implanted an 80-electrode device on the visual cortical surface of a 52-year-old nurse blind from bilateral severe glaucoma and retinal detachment in the left eye. Each electrode was connected by a wire to a radio receiver screwed to the outer bony surface. An oscillator coil was placed above a given receiver in order to activate the receiver via radio frequency and stimulate the cortex via the induced electrical current. With this system, the patient was able to see

 0739-5175/06/$20.00©2006IEEE

[12] K.J. Dormer, "Implantable electronic otologic devices for hearing rehabilitation," in *Handbook of Neuroprosthetic Methods*, W. Finn and P. LoPresti, Eds. Boca Raton, FLA: CRC Press, 2002, pp. 237–260.

[13] J. Georgiou and C. Toumazou, "A 126-μW cochlear chip for a totally implantable system," *IEEE J. Solid-State Circuits*, vol. 40, no. 2, pp. 430–443, 2005.

[14] M.S. Humayun, J.D. Weiland, G.Y. Fujii, R. Greenberg, R. Williamson, J. Little, B. Mech, V. Cimmarusti, G. Van Boemel, G. Dagnelie, and E. de Juan Jr., "Visual perception in a blind subject with a chronic microelectronic retinal prosthesis," *Vision Res.*, vol. 43, no. 24, pp. 2573–2581, 2003.

[15] J.F. Rizzo III, J. Wyatt, J. Loewenstein, S. Kelly, and D. Shire, "Methods and perceptual thresholds for short-term electrical stimulation of human retina with microelectrode arrays," *Invest. Ophthalmol. Vis. Sci.*, vol. 44, no. 12, pp. 5355–5361, 2003.

[16] R. Eckmiller, "Learning retinal implants with epiretinal contacts," *Ophthalmic Res.*, vol. 29, pp. 281–289, 1997.

[17] R. Hornig, T. Laube, P. Walter, M. Velikay-Parel, N. Bornfeld, M. Feucht, H. Akguel, G. Rössler, N. Alteheld, D.L. Notarp, J. Wyatt, and G. Richard, "A method and technical equipment for an acute human trial to evaluate retinal implant technology," *J. Neural Eng.*, vol. 2, no. 1, pp. S129–S134, 2005.

[18] A.Y. Chow, V.Y. Chow, K. Packo, J. Pollack, G. Peyman, and R. Schuchard, "The artificial silicon retina microchip for the treatment of vision loss from retinitis pigmentosa," *Arch. Ophthalmol.*, vol. 122, no. 4, pp. 460–469, 2004.

[19] E. Zrenner, "Will retinal implants restore vision?," *Science*, vol. 295, pp. 1022–1025, 2002.

[20] D. Palanker, A. Vankov, P. Huie, and S. Baccus, "Design of a high-resolution optoelectronic retinal prosthesis," *J. Neural Eng.*, vol. 2, no. 1, pp. S105–S120, 2005.

[21] H. Kanda, T. Morimoto, T. Fujikado, Y. Tano, Y. Fukuda, and H. Sawai, "Electrophysiological studies of the feasibility of suprachoroidal-transretinal stimulation for artificial vision in normal and RCS rats," *Invest. Ophthal. Vis. Sci.*, vol. 45, no. 2, pp. 560–566, 2004.

[22] K. Nakauchi, T. Fujikado, H. Kanda, T. Morimoto, J.S. Choi, Y. Ikuno, H. Sakaguchi, M. Kamei, M. Ohji, T. Yagi, S. Nishimura, H. Sawai, Y. Fukuda, and Y. Tano, "Transretinal electrical stimulation by an intrascleral multichannel electrode array in rabbit eyes," *Graefes Arch. Clin. Exp. Ophthalmol.*, vol. 243, no. 2, pp. 169–174, 2005.

[23] W. Liu, P. Singh, C. DeMarco, R. Bashirullah, M. Humayun, and J. Weiland, "Semiconductor-based implantable microsystems," Chap. 6, in *Handbook of Neuroprosthetic Methods*, W. Finn and P. LoPresti, Ed. Boca Raton, FLA: CRC Press, 2002, pp. 127–161.

[24] W. Liu, K. Vichienchom, M. Clements, S.C. DeMarco, C. Hughes, E. McGucken, M.S. Humayun, E. De Juan, J.D. Weiland, and R. Greenberg, "A neuro-stimulus chip with telemetry unit for retinal prosthetic device," *IEEE J. Solid-State Circuits*, vol. 35, no. 10, pp. 1487–1497, 2000.

[25] W. Liu and M.S. Humayun, "Retinal prosthesis," in *IEEE Int. Solid-State Circuits Conf. Dig. Tech. Papers*, 2004, pp. 218–219.

[26] K. Najafi and K.D. Wise, "An implantable multielectrode array with on-chip signal processing," *IEEE J. Solid-State Circuits*, vol. 21, no. 6, pp. 1035–1986, 1986.

[27] J. Ji, K. Najafi, and K.D. Wise, "A low-noise demultiplexing system for active multichannel microelectrode arrays," *IEEE Trans. Biomed. Eng.*, vol. 38, no. 1, pp. 75–81, 1991.

[28] S.J. Tanghe and K.D. Wise, "A 16-channel CMOS neural stimulating array," *IEEE J. Solid-State Circuits*, vol. 27, no. 12, pp. 1819–1825, 1992.

[29] C. Kim and K.D. Wise, "A 64-site multishank CMOS low-profile neural stimulating probe," *IEEE J. Solid-State Circuits*, vol. 31, no. 9, pp. 1230–1238, 1996.

[30] S.C. DeMarco, W. Liu, P.R. Singh, G. Lazzi, M.S. Humayun, and J.D. Weiland, "An arbitrary waveform stimulus circuit for visual prostheses using a low area multibias DAC," *IEEE J. Solid-State Circuits*, vol. 38, no. 10, pp. 1679–1690, 2003.

[31] Q. Bai and K.D. Wise, "Single-unit neural recording with active microelectrode arrays," *IEEE Trans. Biomed. Eng.*, vol. 48, no. 8, pp. 911–920, 2001.

[32] M. Sivaprakasam, L. Wentai, M.S. Humayun, J.D. Weiland, "A variable range bi-phasic current stimulus driver circuitry for an implantable retinal prosthetic device," *IEEE J. Solid-State Circuits*, vol. 40, no. 3, pp. 763–771, 2005.

[33] T. Kawano, Y. Kato, R. Tani, H. Takao, K. Sawada, and M. Ishida, "Selective vapor-liquid-solid epitaxial growth of micro-Si probe electrode arrays with on-chip MOSFETs on Si (111) substrates," *IEEE Trans. Electron. Devices*, vol. 51, no. 3, pp. 415–420, 2004.

[34] P. Fromherz, "Neuroelectronic interfacing: Semiconductor chips with ion channels, nerve cells, and brain," in *Nanoelectronics and Information Technology*, R. Waser, Ed. New York: Wiley, 2003, pp. 781–810.

[35] B. Eversmann, M. Jenkner, F. Hofmann, C. Paulus, R. Brederlow, B. Holzapfl, P. Fromherz, M. Merz, M. Brenner, M. Schreiter, R. Gabl, K. Plehnert, M. Steinhauser, G. Eckstein, D.S.-Landsiedel, and R. Thewes, "A 128 × 128 CMOS bio-sensor array for extracellular recording of neural activity," *IEEE J. Solid-State Circuits*, vol. 38, no. 12, pp. 2306–2317, 2003.

[36] P.I.-Pastor, I. Mody, and J.W. Judy, "In-vivo EEG recording using a wireless implantable neural transceiver," in *Proc. 1st Int. IEEE EMBS Conf. Neural Eng.*, Capri Island, Italy, 2003, pp. 622–625.

[37] J. Deguchi, T. Watanabe, T. Nakamura, Y. Nakagawa, T. Fukushima, J.-C. Shim, H. Kurino, T. Abe, M. Tamai, and M. Koyanagi, "Three-dimensionally stacked analog retinal prosthesis chip," *Jpn. J. Appl. Phys.*, vol. 43, no. 4B, pp. 1685–1689, 2004.

[38] M. Sawan, Y. Hu, and J. Coulombe, "Wireless smart implants dedicated to multichannel monitoring and microstimulation," *IEEE Circuit Syst. Mag.*, vol. 5, no. 1, pp. 21–39, 2005.

[39] J. Ohta, N. Yoshida, K. Kagawa, and M. Nunoshita, "Proposal of application of pulsed vision chip for retinal prosthesis," *Jpn. J. Appl. Phys.*, vol. 41, no. 4B, pp. 2322–2325, 2002.

[40] K. Kagawa, K. Isakari, T. Furumiya, A. Uehara, T. Tokuda, J. Ohta, and M. Nunoshita, "Pixel design of a pulsed CMOS image sensor for retinal prosthesis with digital photosensitivity control," *Electron. Lett.*, vol. 39, no. 5, pp. 419–420, 2003.

[41] D.C. Ng, K. Isakari, A. Uehara, K. Kagawa, T. Tokuda, J. Ohta, and M. Nunoshita, "A study of bending effect on pulsed frequency modulation based photosensor for retinal prosthesis," *Jpn. J. Appl. Phys.*, vol. 42, no. 12, pp. 7621–7624, 2003.

[42] K. Kagawa, N. Yoshida, T. Tokuda, J. Ohta, and M. Nunoshita, "Building a simple model of a pulse-frequency-modulation photosensor and demonstration of a 128 × 128-pixel pulse-frequency-modulation image sensor fabricated in a Standard 0.35-μm complementary metal-oxide semiconductor technology," *Opt. Rev.*, vol. 11, no. 3, pp. 176–181, 2004.

[43] K. Kagawa, K. Yasuoka, D.C. Ng, T. Furumiya, T. Tokuda, J. Ohta, and M. Nunoshita, "Pulse-domain digital image processing for vision chips employing low-voltage operation in deep-submicrometer technologies," *IEEE J. Select. Topics Quantum Electron.*, vol. 10, no. 4, pp. 816–828, 2004.

[44] T. Furumiya, D.C. Ng, K. Yasuoka, K. Kagawa, T. Tokuda, M. Nunoshita, and J. Ohta, "Functional verification of pulse frequency modulation-based image sensor for retinal prosthesis by in vitro electrophysiological experiments using frog retina," *Biosens. Bioelectron.*, vol. 21, no. 7, pp. 1059–1068, 2006.

[45] A. Uehara, K. Kagawa, T. Tokuda, J. Ohta, and M. Nunoshita, "Back-illuminated pulse-frequency-modulated photosensor using silicon-on-sapphire technology developed for use as epi-retinal prosthesis device," *Electron. Lett.*, vol. 39, no. 15, pp. 1102–1103, 2003.

[46] A. Uehara, Y.-L. Pan, K. Kagawa, T. Tokuda, J. Ohta, and M. Nunoshita, "Micro-sized photo-detecting stimulator array for retinal prosthesis by distributed sensor network approach," *Sens. Actuators A, Phys.*, vol. 120, no. 1, pp. 78–87, 2005.

[47] T. Tokuda, Y.-L. Pan, A. Uehara, K. Kagawa, M. Nunoshita, and J. Ohta, "Flexible and extendible neural interface device based on cooperative multi-chip CMOS LSI architecture," *Sens. Actuators A Phys.*, vol. 122, no. 1, pp. 88–98, 2005.

[48] Y.-L. Pan, T. Tokuda, A. Uehara, K. Kagawa, J. Ohta, and M. Nunoshita, "A flexible and extendible neural stimulation device with distributed multi-chip architecture for retinal prosthesis," *Jpn. J. Appl. Phys.*, vol. 44, no. 4B, pp. 2099–2103, 2005.

[49] L. Li, Y. Hayashida, and T. Yagi, "Temporal properties of retinal ganglion cell responses to local trans retinal current stimuli in the frog retina," *Vision Res.*, vol. 45, no. 2, pp. 263–273, 2005.

[50] A.P. Chu, K. Morris, R.J. Greenberg, and D.M. Zhou, "Stimulus induced pH changes in retinal implants," in *Proc. 26th Int. Conf. IEEE EMBS*, San Francisco, California, U.S.A., 1–5 Sept. 2004, pp. 4160–4162.

[51] T.L. Rose and L.S. Robblee, "Electrical stimulation with Pt electrodes. VIII. Electrochemically safe charge injection limits with 0.2 ms pulses," *IEEE Trans. Biomed. Eng.*, vol. 37, no. 11, pp. 1118–1120, 1990.

[52] S.B. Brummer and M.J. Turner, "Electrical stimulation with Pt electrodes: II—estimation of maximum surface redox (theoretical non-gassing) limits," *IEEE Trans. Biomed. Eng.*, vol. 24, no. 5, pp. 440–443, 1977.

[53] S.B. Brummer and M.J. Turner, "Electrical stimulation with Pt electrodes: I. A method for determination of 'real' electrode areas," *IEEE Trans. Biomed. Eng.*, vol. 24, no. 5, pp. 436–439, 1977.

[54] J.D. Weiland and D.J. Anderson, "Chronic neural stimulation with thin-film, Iridium Oxide electrodes," *IEEE Trans. Biomed. Eng.*, vol. 47, no. 7, pp. 911–918, 2000.

[55] S.F. Cogan, T.D. Plante, J. Ehrlich, "Sputtered iridium oxide films (SIROFs) for low-impedance neural stimulation and recording electrodes," in *Proc. 26th Int. Conf. IEEE EMBS*, San Francisco, California, U.S.A., 1–5 Sept. 2004, pp. 4153–4156.

[56] W. Yang, "A wide-dynamic-range, low-power photosensor array," in *IEEE Int. Solid-State Circuits Conf. Dig. Tech. Papers*, 1994, pp. 230–231.

[57] M. Mazza, P. Renaud, D.C. Bertrand, and A.M. Ionescu, "CMOS Pixels for Subretinal Implantable Prosthesis," *IEEE Sens. J.*, vol. 5, no. 1, pp. 32–37, 2005.

IOP PUBLISHING JOURNAL OF NEURAL ENGINEERING
J. Neural Eng. 4 (2007) S85–S91 doi:10.1088/1741-2560/4/1/S10

Laboratory investigation of microelectronics-based stimulators for large-scale suprachoroidal transretinal stimulation (STS)

J Ohta[1], T Tokuda[1], K Kagawa[1], S Sugitani[1], M Taniyama[1], A Uehara[2], Y Terasawa[2], K Nakauchi[3], T Fujikado[3] and Y Tano[4]

[1] Graduate School of Materials Science, Nara Institute of Science and Technology, 8916-5 Takayama, Ikoma, Nara 630-0101, Japan
[2] Vision Institute, Nidek Co., Ltd, 73-1 Hamacho, Gamagori, Aichi, Japan
[3] Department of Applied Visual Science, Osaka University Graduate School of Medicine, 2-2 Yamadagaoka, Suita, Osaka, Japan
[4] Department of Ophthalmology, Osaka University Graduate School of Medicine, 2-2 Yamadagaoka, Suita, Osaka, Japan

E-mail: ohta@ms.naist.jp

Received 3 October 2006
Accepted for publication 14 December 2006
Published 26 February 2007
Online at stacks.iop.org/JNE/4/S85

Abstract

This paper describes the technological developments underlying the realization of a reliable and reproducible microchip-based stimulator with a large number of stimulus electrodes. A microchip-based stimulator with over 500 electrodes for suprachoroidal transretinal stimulation (STS) is proposed in this paper, and an example is presented. To enhance reliability and reproducibility for such a large array, we introduce a flip-chip bonding technique and place microchips on the reverse side of a substrate. A square microchip of size 600 μm was fabricated using 0.35 μm standard CMOS process technology. Twelve microchips were flip-chip bonded on a polyimide substrate through Au bumps. To evaluate the feasibility of the proposed device, we successfully fabricated a stimulator with 12 microchips and 118 electrodes made of Pt/Au bumps, and demonstrated their operation in a saline solution for 2 weeks. Also, to evaluate the device operation *in vivo*, a stimulator with one active IrO_x electrode was implanted into the scleral pocket of a rabbit and electrical evoked potential (EEP) signals with a threshold of 100 μA were obtained. We also fabricated a simulator with 64 microchips that has 576 electrodes (9 electrodes in a microchip times 64 microchips).

(Some figures in this article are in colour only in the electronic version)

1. Introduction

Several types of intraocular retinal prostheses for blind patients have been reported [1–7]. With the exception of [5], most have been characterized by a small number of electrodes. Although more than 1000 electrodes would be preferable for realizing better vision using a retinal prosthesis, we are faced with the issue of interconnection between electrodes and external lead wires when increasing the number of electrodes.

Figure 1 illustrates the methods used to realize a stimulus electrode array. The direct connection method, which is commonly used in retinal prosthetic devices, is shown in figure 1(a), where each electrode is directly connected to a lead wire. A more sophisticated method is shown in figure 1(b), where a multiplexer is employed to reduce the number of external lead wires. If the number of electrodes is increased further, it would be difficult to connect electrodes to the multiplexer due to the number of wires.

 © 2007 IOP Publishing Ltd Printed in the UK

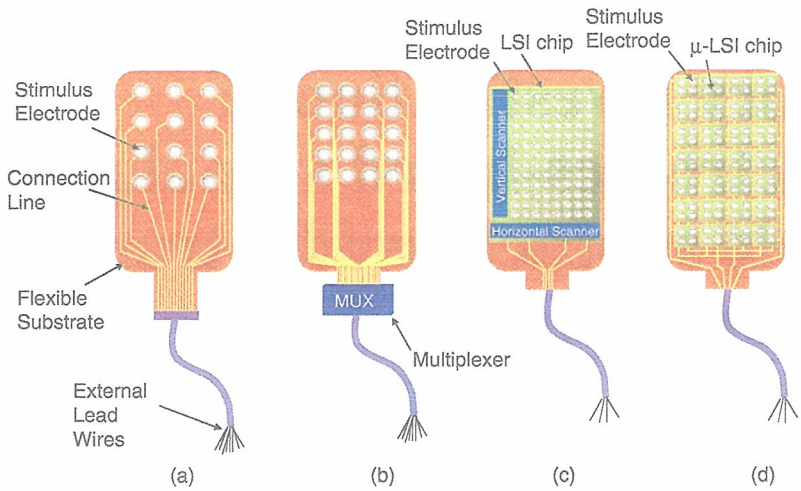

Figure 1. Illustration of several methods to realize connections between electrodes and external lead wires. (a) Direct connections between electrodes and lead wires. (b) Introducing a multiplexer to reduce the number of external lead wires. (c) An LSI chip introduced for scanning circuits. (d) Our proposed method using microchips.

It is thus preferable to introduce a large-scale integration (LSI) chip in the stimulator, as shown in figure 1(c). The LSI chip enables scanning circuits (scanners) to be integrated to reduce the number of wires. Random access can be implemented using decoder circuits instead of scanners. However, it is difficult to use an LSI chip in a retinal stimulator device. Specifically, for implantation, an LSI-based stimulator should be thin and flexible to accommodate the eye and to avoid damaging tissue. However, silicon is rigid and decreasing the thickness of the LSI chip increases the risk of breakage.

To solve this issue, we have already developed a novel smart stimulator that consists of a number of LSI-based microchips distributed on a flexible substrate, as shown in figure 1(d) [10–12]. Each microchip has several stimulus electrodes, which can be externally controlled to turn on and off through an external control circuit. In addition to resolving the interconnections issue, LSI-based stimulators offer several advantages for signal processing. To facilitate flexibility, we place several microchips on a substrate in a distributed manner.

In this paper, we propose a new structure for realizing a large electrode array. This new structure offers improved extendibility and sealing characteristics in a biological environment in comparison with our previously proposed stimulator [11]. This latest stimulator was primarily developed for suprachoroidal transretinal stimulation (STS) applications [8, 9], although it has other potential applications, such as subretinal stimulation. In addition, STS has been applied recently to RP (retinitis pgimentosa) patients [7].

This paper is organized as follows. First, we describe the design and fabrication process of the stimulator for STS. Next, the experimental results of the simulator are demonstrated. Finally, a stimulator approaching a 1000-electrode array is discussed.

2. Design and fabrication of the stimulator

2.1. Microchip design

The microchip architecture is almost the same as in [10]; it has nine stimulation pads and four input lines, including the power supply lines. However, the chip in this paper has been improved to accommodate an increased number of microchips in the stimulator. The circuits of the microchip are briefly described below. A detailed description of the integrated circuits will appear in [13].

A block diagram of the chip is shown in figure 2. Each stimulation pad is assigned a unique 4-bit address that can selectively activate one of the nine electrodes on a microchip. The four input lines are VDD, GND, CTLR and STIM. The VDD and GND lines are used for the power supply (VDD = 5 V), and control and stimulation can be achieved with only two lines: CTLR and STIM. Each of the stimulation electrodes can be selected with the number of the pulses applied on the CTLR line. This is achieved by the microchip counting the pulses applied on the CTLR line using a 10-bit address buffer. As shown in figure 2, the lower 4 bits of the address buffer are used for electrode selection and the upper 6 bits are used for chip identification. The stimulation current is provided from outside of the chip and fed into the STIM terminal. Because a precise current source can be used, the charge balance is maintained. Therefore, a capacitor for charge balance and preventing the flow of unintentional dc current to the tissues is not employed in the present design.

One of the stimulation electrodes is selected depending on the value in the lower 4 bits of the address buffer. The 6-bit address space for microchips facilitates the control of an arbitrary number of microchips (up to 64) using only one set of input lines. Consequently, the multi-chip stimulation device platform can configure a 64-chip device with 576 stimulation electrodes. To ensure flexibility, the microchip array is assembled at a pitch of 1000–1200 μm.

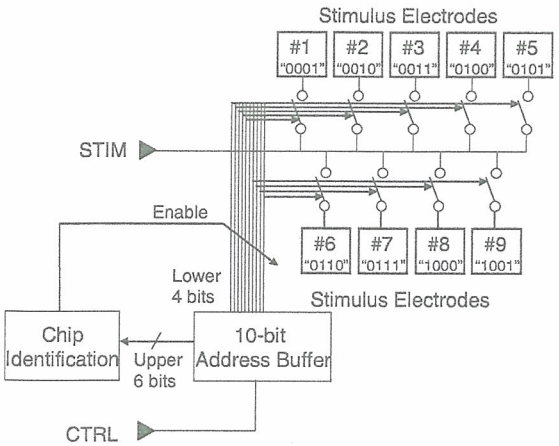

Figure 2. Block diagram of the microchip. The 4-digit number in each stimulus electrode refers to the number assigned to the electrode.

The microchips are diced from a mother chip, which is fabricated using 0.35 μm standard CMOS technology. The mother chip contains 16 microchips. Figure 3 shows microphotographs of a mother chip and a microchip measuring 600 μm $\times$ 600 μm.

2.2. *Stimulator design*

To enhance the extendibility and reliability of the stimulator for large array sizes, we propose a new stimulator design that places the microchips on the reverse side of a flexible substrate by a process called flip-chip bonding. Flip-chip bonding has not been used in the design of previous stimulators [10, 11]. The detailed fabrication process has been submitted for publication in [13]. The proposed stimulator is illustrated in figure 4. For clarity in the figure, the microchips have been placed on the substrate, but in use they are placed on the reverse side of the substrate and thus cannot be seen.

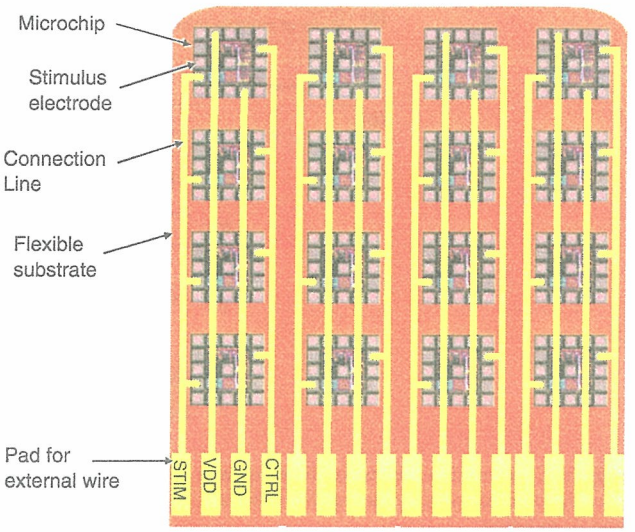

Figure 4. Illustration of the stimulator. 4 $\times$ 4 microchips are placed on a substrate. Four vertical lines for VDD, GND, STIM and CTRL connect four microchips.

For extendibility, the microchips are connected to each other such that a column can be extended vertically. Consequently, the stimulator can accommodate more microchips. All of the connection wires are placed on the reverse side of the substrate; no wires connecting microchips are necessary, which means that the stimulator is more reliable compared with previous stimulators, in which microchips were connected via wires [11].

2.3. *Fabrication process of the stimulator*

We designed and fabricated the arrayed microchip using one die. The fabrication process is shown in figure 5 and described as follows. First, grooves for separating each microchip are formed on the die. Then, connection bumps for flip-chip bonding are formed on the pads of the microchips. We use

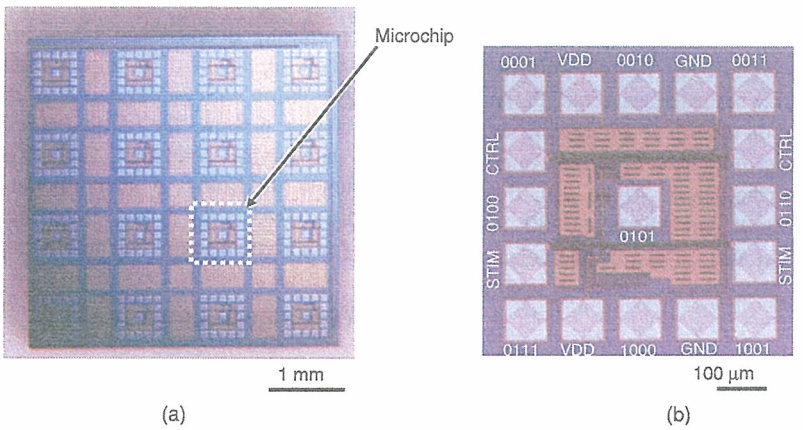

Figure 3. Microphotographs of (a) the fabricated mother chip and (b) a diced microchip. The four-digit number in (b) is the same as that shown in figure 2.

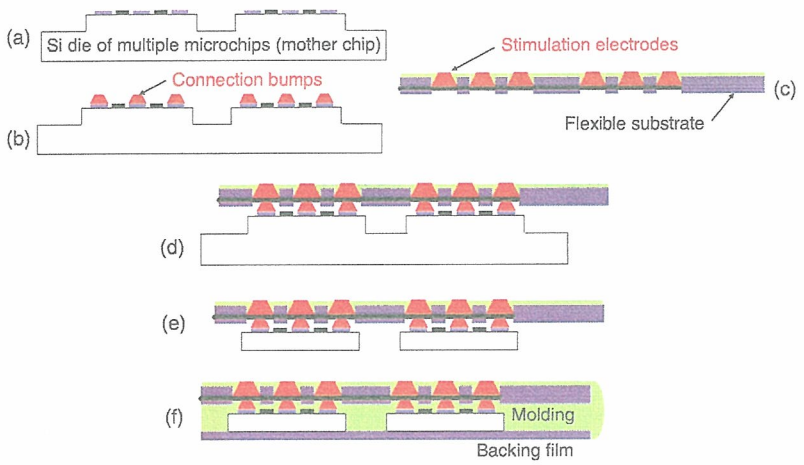

Figure 5. Fabrication process of the stimulator. (a) Grooving for separation, (b) formation of connection bumps, (c) formation of stimulation electrodes on the flexible substrate, (d) flip-chip bonding with the Si mother chip and flexible substrate, (e) microchip separation and (f) molding.

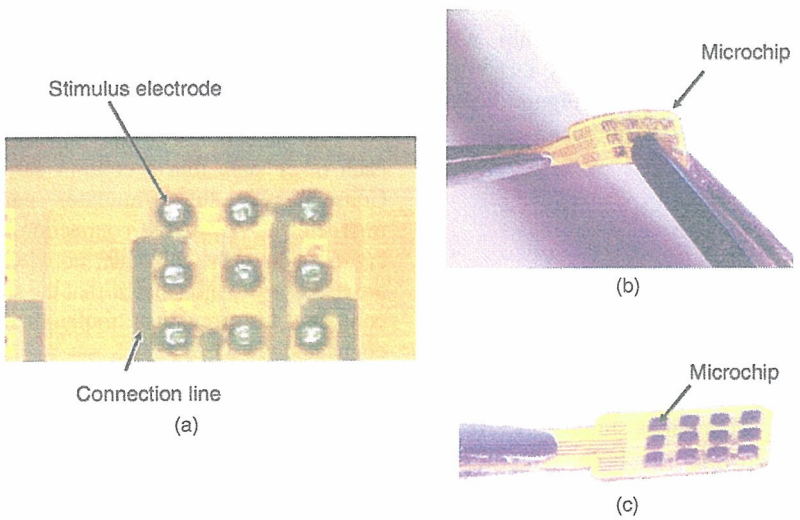

Figure 6. Microphotographs of the fabricated stimulator. (a) Close-up view of the upper surface of the fabricated stimulator. (b) Upper surface view of the stimulator to show that it can easily be bent. (c) Reverse surface view of the stimulator to show the microchips flip-chip-bonded on the substrate.

gold ball bumps as the connection bumps. Next, the die is bonded onto the reverse side of the flexible patterned substrate by the flip-chip bonding technique. A polyimide film was used for the flexible substrate in the experiments. Pt/Au bump electrodes [10] are formed on the top of the flexible substrate, each of which measures approximately 75 m$\mu\phi$. An electrode consists of a Pt top part (diameter: 70–80 μm, thickness: 20–40 μm) and a Au bottom part (diameter: 80–100 μm, thickness: 10–40 μm). The top surface of each electrode is flattened by the tamping process (i.e., pressing with a solid material).

The bottom of the die is then ground to separate each microchip completely before molding with epoxy resin and a backing film made of Teflon film. The molding material, epoxy resin, is used for sealing against moisture, which is evaluated *in vitro* in the short term, as mentioned in section 3.1. We have not yet confirmed the long-term sealing performance and biocompatibility for individual materials, although we are preparing to introduce a biocompatible epoxy resin for the molding layer. To improve the sealing performance, encapsulation with parylene is also under examination.

Figure 6 shows the fabricated stimulator. The stimulator has acceptable thickness (approximately 250 μm) and sufficient flexibility to accommodate an eyeball, which is demonstrated in the *in vivo* experiment in section 3.2. Since there are 16 microchips, the total number of electrodes is 144.

3. Fundamental operations

3.1. In vitro operation

The fabricated stimulator with Pt/Au electrodes was tested in a saline solution for several pulse conditions. Figure 7 summarizes the experimental results, which show that the stimulator can operate properly in a saline solution. The

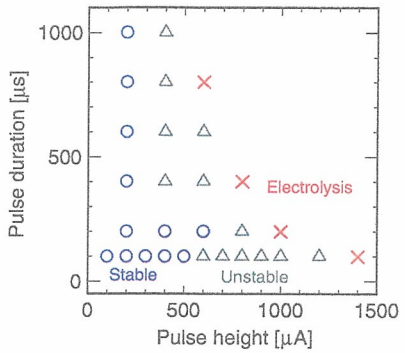

Figure 7. Operating region of the stimulator in saline solution. ○: stable condition; △: unstable condition where electrolysis occasionally occurred after some trials; ×: irreversible condition where electrolysis occurred, that is, gas bubbling was observed. Pulse is cathodic-first biphasic and cathodic, anodic and interpulse durations are the same. The repetition rate is 1 kHz.

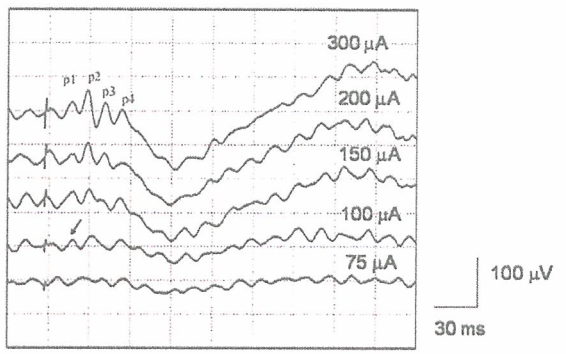

Figure 8. EEP signals, showing the parameters of the pulse current amplitude for a duration of 0.5 ms. The arrow indicates the p1 peak at the threshold.

pulse parameters used are described in the figure caption. We also confirmed that the maximum charge capacity of our electrode (Pt) is estimated approximately as 1 mC cm^{-2}, which is three times larger than the values cited in the literature [14]. This is presumably due to neglecting the surface roughness factor to estimate the charge capacity in our electrodes, and needs further studies. Another experiment demonstrated that the stimulator could operate for more than 2 weeks with a cathodic-first biphasic pulse of 200 μA in amplitude for both cathodic and anodic pulses with a duration of 200 μs for both pulses and interpulses at the frequency of 1 kHz. The *in vitro* results demonstrate that, in the 2 weeks of testing, the molding was leak-tight and the electrodes worked well without damage. The long-term evaluation, however, is a future issue.

3.2. *In vivo* operation

We then conducted an *in vivo* experiment in which we implanted the fabricated stimulator into the scleral pocket of a rabbit eye using an operation procedure similar to that described in [9]. In this experiment, a dummy silicon chip, which was the same size as the microchip, was used and IrO_x was formed on the Pt electrode to increase the charge capacity and ensure the effective stimulation in an *in vivo* environment. A dummy chip is useful for evaluating fundamental characteristics such as bending in the tissue, stimulation performance with a simple operation, and so on, in a first trial. The values of the charge capacity of the Pt and IrO_x used here are in the range of values cited in the literature [14]. The size of the electrode was the same as the stimulator that was described in the previous section. The method of recording EEP from anesthetized rabbit cortex with the stimulator in STS is as follows.

Implantation of the recording electrodes. The rabbit was anesthetized with an intramuscular injection of ketamine hydrochloride (50 mg kg^{-1}) and xylazine hydrochloride (5 mg kg^{-1}), which provided a stable anesthesia for more than 2 h. The recording electrode was a stainless-steel screw. The electrode was screwed into the skull at the area of the visual

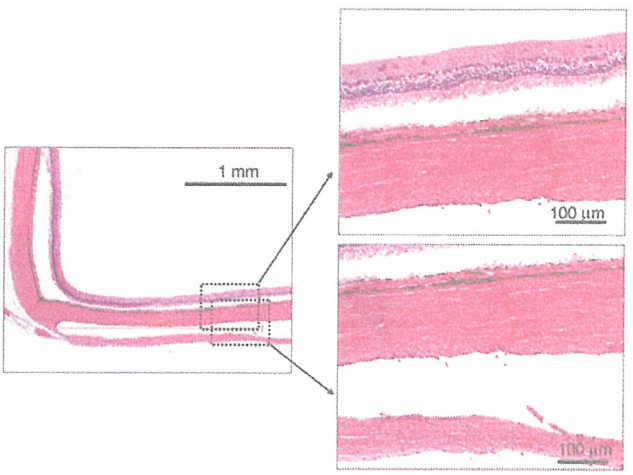

Figure 9. Histology of the retina and sclera around the electrode array.

cortex to a depth of 4 mm so that the tip touched the dura mater. The reference electrode was screwed at the bregma.

Implantation of the stimulating electrodes. The rabbit eye was proptosed and draped with sterilized rubber cloth. After cutting the ventral conjunctiva, the exposed inferior rectus and inferior oblique muscles were cut at the insertion. Then, a 4 × 4 mm scleral pocket was made over the visual streak, which is located 10 mm dorsal to the lower corneal limbus. The electrode was inserted into that pocket and fixed with a 5-0 Dacron suture. A return electrode was inserted into the vitreous cavity. A scleral hole was made at 1 mm from the limbus with a 30-gauge needle. The electrode wire was inserted 3 mm into the vitreous and fixed by an 8-0 Vicryl suture, and a silicone tube was fixed by a 5-0 Dacron suture on the sclera.

Stimulation parameters. Monophasic 0.5 ms duration pulses with anodic polarity were used to elicit the EEPs. The stimulus currents were changed to determine threshold currents, but they did not exceed 500 μA. A power generator (A-365R; World Precision Instruments Inc., Sarasota, FL, USA) was connected to an electronic pulse generator (Stimulator SEN-7203, Nihon Kohden, Shinjyuku, JAPAN).

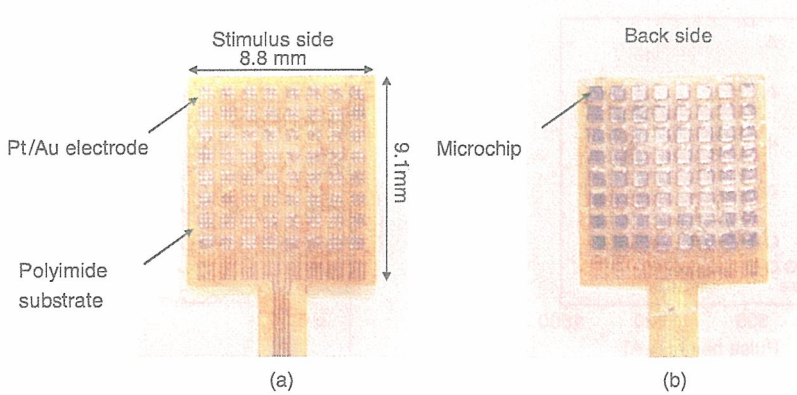

Figure 10. Photographs of the fabricated stimulator with 576 Pt/Au electrodes. (a) Upper surface view to show the 576 stimulus electrodes. (b) Reverse surface view to show the 16 microchips flip-chip bonded on the polyimide substrate.

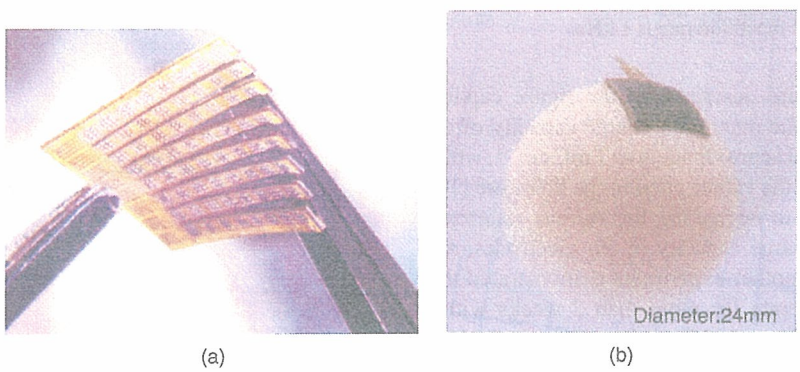

Figure 11. Photographs of the 576-electrode stimulator with vertical cutting slits. (a) By virtue of the vertical slits, the stimulator can be bent in any direction, and (b) can be fitted to a ball with the same diameter as the human eye.

Recording methods. The visual evoked potentials (VEPs) and EEPs were recorded with the Neuropac (KD-019A, Nihon Kohden) system. A flash bulb (1.2 J) was placed 15 cm from the cornea. The responses to 20 stimuli were averaged for the VEP. Then, 20 to 30 EEP responses were averaged.

Figure 8 shows the EEP experimental results, where we conclude that 'p1' is the EEP signal from the ganglion cells because of the latency of the signal. The p1 peak and other peaks after p1 are discussed in detail in [9]. From p1, the threshold is approximately 100 μA (<1 mC cm^{-2}), which is considered adequate for the charge capacity of the electrode (1–4 mC cm^{-2} [14]).

The electrode array was implanted for 2 weeks after stimulation for 1 h with the following pulse parameters: an anodic pulse with a height of 1 mA, duration of 0.5 ms and frequency of 20 Hz. As shown in figure 9, histological examination revealed that the stimulator caused only minor damage to the retinal tissue after 2 weeks.

4. A 1000-electrode stimulator

In this section, we discuss a stimulator consisting of an array approaching 1000 electrodes. In the present stimulator, the number of stimulus electrodes can be increased up to 576; the 6-bit address for microchips can be assigned to 64 microchips, and since nine electrodes can be accommodated by each of the 64 microchips, a total of 576 electrodes can be integrated into the stimulator. It is possible to increase the number of electrodes by increasing the address bit from 6 bits to 7 bits; a 7-bit address can assign 128 microchips, which would result in 1152 electrodes in the stimulator. Another way to reach a 1000-electrode stimulator is to use two sets of the 576-electrode stimulator, thereby realizing 1152 electrodes. We fabricated a mockup stimulator, in which dummy Si chips without integration circuits were used instead of microchips. Sixty-four chips were placed on the substrate to give 576 stimulus electrodes on the stimulator, as shown in figure 10. The size of the stimulator is 8.8 mm × 9.1 mm.

By introducing vertical slits in the stimulator, it can be bent, even if the size of the stimulator is as large as that shown in figure 11(a). Figure 11(b) shows that a large stimulator such as this can be fitted to a ball with the same diameter as that of a human eye (24 mm).

Although this stimulator was designed for demonstration purposes, we believe that this method would be effective for producing large-scale STS stimulators.

5. Conclusions

We have proposed and fabricated a flip-chip type stimulator for a large number of stimulations for STS. Better extendibility

and reliability are demonstrated compared with previously proposed stimulators, and as many as 576 simulation electrodes can be realized in the fabricated device. The operation of the fabricated stimulator was tested in a saline solution and found to function within safe operation limits. A stimulator with one active IrO_x electrode on a dummy Si microchip was also implanted in the scleral pocket of a rabbit, where it operated for 2 weeks. By using the stimulator, EEP signals with thresholds of 100 μA were observed. With the intention of fabricating a 1000-electrode stimulator, we fabricated a 576-electrode stimulator with vertical slits that can be accommodated by a human eyeball.

Acknowledgments

The authors would like to thank Professor H Tashiro of Kyushu University, M Ozawa, K Shodo, H Kanda and N Tsunematsu of Nidek Co. Ltd for their valuable discussions. This work was partly supported by the New Energy Development Organisation (NEDO) of Japan ('Artificial Vision System' Project) and by a Health and Labour Sciences Research Grant, Japan.

References

[1] Humayun M S *et al* 2003 Visual perception in a blind subject with a chronic microelectronic retinal prosthesis *Vis. Res.* **43** 2573–81

[2] Liu W and Humayun M S 2004 Retinal prosthesis *IEEE Int. Solid-State Circuits Conf. Dig. Technical Papers* pp 218–9

[3] Rizzo J F III, Wyatt J, Loewenstein J, Kelly S and Shire D 2003 Methods and perceptual thresholds for short-term electrical stimulation of human retina with microelectrode arrays *Invest. Ophthalmol. Vis. Sci.* **44** 5355–61

[4] Hornig R *et al* 2005 A method and technical equipment for an acute human trial to evaluate retinal implant technology *J. Neural Eng.* **2** S129–34

[5] Chow A Y, Chow V Y, Packo K, Pollack J, Peyman G and Schuchard R 2004 The artificial silicon retina microchip for the treatment of vision loss from retinitis pigmentosa *Arch. Ophthalmol.* **122** 460–9

[6] Zrenner E, Besch D, Bartz-Schmidt K U, Gekeler F, Gabel V P, Kuttenkeuler C, Sachs H, Sailer H, Wilhelm B and Wilke R 2006 Subretinal chronic multi-electrode arrays implanted in blind patients *Invest. Ophthalmol. Vis. Sci.* **47** E-Abstract 1538

Zrenner E 2006 Subretinal chronic multi-electrode arrays implanted in blind patients *Abstract Book of Shanghai Int. Conf. Physiological Biophysics (Shanghai)* p 147

[7] Kamei M, Fujikado T, Kanda H, Morimoto T, Nakauchi K, Sakaguchi H, Ikuno Y, Ozawa M, Kusaka S and Tano Y 2006 Suprachoroidal-transretinal stimulation (STS) artificial vision system for patients with retinitis pigmentosa *Invest. Ophthalmol. Vis. Sci.* **47** E-Abstract 1537

[8] Kanda H, Morimoto T, Fujikado T, Tano Y, Fukuda Y and Sawai H 2004 Electrophysiological studies of the feasibility of suprachoroidal-transretinal stimulation for artificial vision in normal and RCS rats *Invest. Ophthalmol. Vis. Sci.* **45** 560–6

[9] Nakauchi K *et al* 2005 Transretinal electrical stimulation by an intrascleral multichannel electrode array in rabbit eyes *Graefe's Arch. Clin. Exp. Ophthalmol.* **243** 169–74

[10] Ohta J, Tokuda T, Kagawa K, Furumiya T, Uehara A, Terasawa Y, Ozawa M, Fujikado T and Tano Y 2006 Silicon LSI-based smart stimulators for retinal prosthesis *IEEE Eng. Med. Biol. Mag.* **25** 47–59

[11] Tokuda T, Pan Y-L, Uehara A, Kagawa K, Nunoshita M and Ohta J 2005 Flexible and extendible neural interface device based on cooperative multi-chip CMOS LSI architecture *Sensors Actuators* A **122** 88–98

[12] Uehara A, Pan Y-L, Kagawa K, Tokuda T, Ohta J and Nunoshita M 2005 Micro-sized photo detecting stimulator array for retinal prosthesis by distributed sensor network approach *Sensors Actuators* A **120** 78–87

[13] Tokuda T, Sugitani S, Taniyama M, Uehara A, Terasawa Y, Kagawa K, Nunoshita M, Tano Y and Ohta J 2007 Fabrication and validation of a multi-chip neural stimulator for *in vivo* experiments toward retinal prosthesis *Japan. J. Appl. Phys.* **46** at press

[14] Weiland J D, Liu W and Humayun M S 2005 Retinal prosthesis *Annu. Rev. Biomed. Eng.* **7** 361–401

J Artif Organs (2006) 9:263–266
DOI 10.1007/s10047-006-0352-1

© The Japanese Society for Artificial Organs 2006

BRIEF COMMUNICATION

Yasuo Terasawa, MS · Hiroyuki Tashiro, MS
Akihiro Uehara, PhD · Tohru Saitoh, BS
Motoki Ozawa, MS · Takashi Tokuda, PhD
Jun Ohta, PhD

The development of a multichannel electrode array for retinal prostheses

Abstract The development of a multielectrode array is the key issue for retinal prostheses. We developed a 10 × 10 platinum electrode array that consists of an 8-μm polyimide layer sandwiched between 5-μm polymonochloro-para-xylylene (parylene-C) layers. Each electrode was formed as a 30-μm-high bump by Pt/Au double-layer electroplating. We estimated the charge delivery capability (CDC) of the electrode by measuring the CDCs of two-channel electrode arrays. The dimensions of each electrode of the two-channel array were the same as those of each electrode formed on the 10 × 10 array. The results suggest that for cathodic-first (CF) pulses, 80% of electrodes surpassed our development target of 318 μC/cm^2, which corresponds to the charge density of pulses of 500 μs duration and 200 μA amplitude for a 200-μm-diameter planar electrode.

Key words Visual prosthesis · Electrode · Charge delivery capability

Introduction

In spite of recent advances in medicine, there is no effective treatment for blindness. Recently, it has been shown that a certain percentage of retinal cells survive even in the retina of a totally blind eye,[1,2] which has encouraged the development of retinal prostheses. Chow[3,4] and Zrenner[5,6] pioneered subretinal prostheses that implant the electrode array inside the subretinal space, followed by the development of epiretinal prostheses.[7–10] We are trying to develop suprachoroidal prostheses, in which the electrode array is positioned in neither the epiretinal nor the subretinal space but inside the sclera.[11] Compared with other aproaches, our suprachoroidal approach is advantageous because electrodes can be implanted by relatively low invasive surgery.[12] Therefore, our electrode array must satisfy the following two criteria. First, the size of the electrode array should be small enough to be inserted into the scleral flap. Second, each electrode should be able to deliver enough charge to stimulate retinal cells safely. In addition, our in vivo preliminary study has shown that a convex electrode is preferable to a planar electode. The fabrication of a convex electrode is difficult compared with conventional micromachining-based planar electrodes.[13,14]

It has been reported that the minimum threshold current amplitude is 100 μA for cathodic-first (CF) 500-μs-duration pulses to evoke electrically-evoked cortical potentials in rats.[11] We have assumed a safety coefficient of two for the current amplitude; therefore, the electrode should be able to inject current pulses of 200 μA amplitude and 500 μs duration safely. The charge delivery capability (CDC) of platinum is reported to be in the range of 300–350 μC/real cm^2, depending on the pulse polarity.[15] Assuming a CDC for platinum of 350 μC/cm^2, a 191-μm-diameter electrode is necessary to inject a pulse of 200 μA amplitude and a 500 μs width. This is why we set our development target to be 200-μm-diameter electrodes that can deliver CF biphasic pulses of 200 μA amplitude and 500 μs duration, which is equivalent to a charge density of 318 μC/cm^2. In this article we report on a fabrication process that accommodates convex electrodes and on the CDC measurements of our multichannel electrodes designed for intrascleral implantation. Then we discuss whether our electrodes satisfy our development target.

Received: January 4, 2006 / Accepted: August 16, 2006

Y. Terasawa (✉) · A. Uehara · T. Saitoh · M. Ozawa
Vision Institute, Nidek Co, Ltd, 73-1 Hama-cho, Gamagori 443-0036, Japan
Tel. +81-533-68-1815; Fax +81-533-68-1816
e-mail: yasuo_terasawa@nidek.co.jp

H. Tashiro
Department of Medicine, Kyushu University, Fukuoka, Japan

T. Tokuda · J. Ohta
Graduate School of Materials Science, Nara Institute of Science and Technology, Nara, Japan

Materials and methods

The micromachining process is shown in Fig. 1. First, polyimide varnish was spun on a stainless plate, which served as a sacrificial layer. Next, 20/1000-nm Ti/Au layers were sputtered and patterned. At electrode sites, 219-μm-diameter islands were formed. The center-to-center distance between two electrodes was 400 μm. The minimum line/space was 9 μm/10 μm because we had to arrange nine lines at most between two electrodes. Then 25-μm-thick gold bumps were formed at electrode sites as a 10 × 10 array by electroplating, followed by 1 μm platinum deposition. We chose electroplating to form the electrodes because of its compatibility with the micromachining process; another method based on the stud bump technique has been proposed.[16] The maximum width of the electrode array was 4.2 mm. After photoresist removal, the surfaces of electrode arrays were coated with 5 μm polymonochloro-para-xylylene (Parylene-C, Speciality Coating Systems, Indianapolis, IN, USA). Parylene-C was chosen because its conformal coating layer has a low water vapor transmission rate and also acts as an insulation layer.[17] In addition, Parylene is known to be biocompatible,[18] can be deposited at room temperature, and is easily removed by laser ablation or dry etching.[19] Next, the stainless plate was dissolved to separate the electrode arrays and the backs of the electrode arrays were coated with 5 μm of Parylene-C. Finally, each electrode array was cut out and the tip of each electrode was laser ablated to expose the 200-μm-diameter platinum. We also fabricated a two-channel electrode array in parallel to measure the CDC because the 10 × 10 electrode array was designed to be integrated with a multiplex chip and it was difficult to access individual electrodes electrically. The size and structure of the electrodes on the two-channel array were the same as those of electrodes formed on the 10 × 10 electrode array. We assume that current pulses will be applied serially, i.e., multiple electrodes will not be activated simultaneously. Therefore, measuring the CDCs of two-channel electrode arrays is equivalent to the CDC measurement of 10 × 10 electrode arrays.

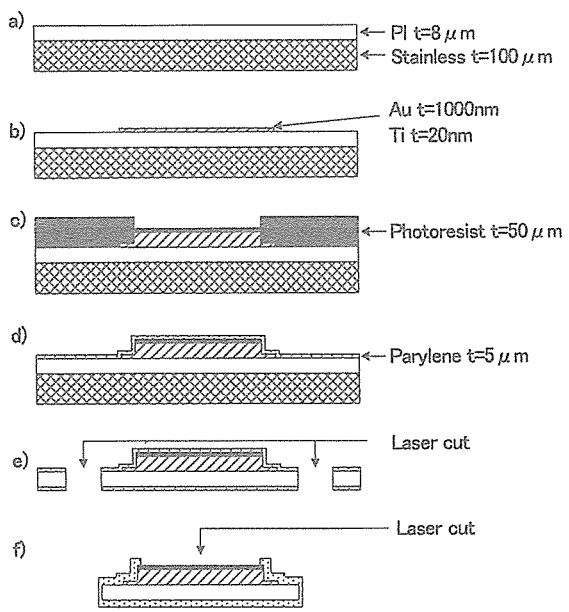

Fig. 1a–f. Micromachining of electrode arrays. **a** Spinning polyimide (*PI*) on a stainless plate; **b** metal deposition and patterning; **c** photoresist patterning and electroplating of Pt on Au; **d** parylene deposition after photoresist removal; **e** stainless plate removal, parylene coating of the back, and laser cutting; **f** second parylene deposition and parylene removal from Pt. *t*, thickness

A custom-built stimulator was used to measure the CDC of the electrode. CDC is defined as the maximum charge delivered under the condition that the electrode potential does not exceed the water window. A detailed evaluation procedure is described elsewhere.[20] In brief, symmetrical biphasic current pulses of 0.5 ms duration and 50 Hz repetition frequency were applied between the Pt bump electrode and a large (>2 cm^2) Pt plate for 15 min in 0.01 M phosphate-buffered saline (PBS). A silver/silver chloride reference electrode was used to measure the electrode potential. The charge balance was achieved by the discharge of a 1-μF capacitor in series with a 100-Ω current measuring resistor. The output terminals of the stimulator were electrically shorted 50 μs after outputting the biphasic pulse for 50 μs to discharge the capacitor. While applying pulses, the transients of the electrode potentials were recorded and examined if electrode potentials were kept within the water window while current pulses were applied. The instantaneous voltage drop at the onset of the current pulse (iR drop) was corrected in real time by subtracting the iR drop from the measured electrode potential. The iR drop was calculated with an oscilloscope by multiplying the cell constant and the measured current. A total of 128 potential transients were continuously captured, and averaged waveforms were recorded. The temperature of the saline was kept at 37°C and the saline was continuously bubbled with a mixture of gases (O_2:CO_2:N_2 = 6%:5%:89%). Three two-channel electrodes were used in this study.

Results

Fabrication

We succeeded in micropatterning Ti/Au by a conventional wet etching process. The parylene removal by laser ablation was also performed successfully, but we sometimes observed cracks on the surfaces of electrodes when the energy of the laser pulse was greater than 1 mJ/pulse. Black scorch marks were observed on the surface of electrodes after laser ablation, which did not disappear even when helium gas was applied as an assist gas. Ar plasma treatment could remove the scorch marks, but this sometimes resulted in delamination between the Parylene and the polyimide.

CDC measurement

The measured CDCs are summarized in Table 1. The average CDC was 62.1 μC/cm^2 for anodic-first (AF) pulses and

Conclusion

We succeeded in fabricating a 10 × 10 bump-shaped electrode array onto a flexible substrate. CDC measurements of the electrodes indicated that 80% of electrodes (four of five) performed beyond 318 $\mu C/cm^2$, which was our development target. The fact that there was little difference between measured and target CDCs suggested the necessity of enhancing the charge delivery capability of electrodes.

Acknowledgments This work was supported by the New Energy Development Organization (NEDO) of Japan.

References

1. Santos A, Humayun MS, de Juan E Jr, Greenberg R, Marsh MJ, Klock IB, Milam AH. Preservation of the inner retina in retinits pigmentosa. A morphometric analysis. Arch Ophthalmol 1997;115: 511–515
2. Kim SY, Sadda S, Pearlman J, Humayun MS, de Juan E Jr, Melia BM, Green WR. Morphometric analysis of the macula in eyes with disciform age-related macular degeneration. Retina 2002;22:471–477
3. Chow AY, Chow VY. Subretinal electrical stimulation of the rabbit retina. Neurosci Lett 1997;225:13–16
4. Chow AY, Pardue MT, Chow VY, Peyman GA, Liang C, Perlman JI, Peachey NS. Implantation of silicon chip microphotodiode arrays into the cat subretinal space. IEEE Tran Neural Sys Rehab Eng 2001;9:86–95
5. Zrenner E, Stett A, Weiss S, Aramant RB, Guenther E, Kohler K, Miliczek KD, Seiler MJ, Haemmerle H. Can subretinal microphotodiodes successfully replace degenerated photoreceptors? Vision Res 1999;39:2555–2567
6. Stett A, Barth W, Weiss S, Haemmerle H, Zrenner E. Electrical multisite stimulation of the isolated chicken retina. Vision Res 2000;40:1785–1795
7. Humayun MS, de Juan E Jr, Weiland JD, Dagnelie G, Katona S, Greenberg R, Suzuki S. Pattern electrical stimulation of the human retina. Vision Res 1999;39:2569–2576
8. Humayun MS, Weiland JD, Fujii GY, Greenberg R, Williamson R, Little J, Mech B, Cimmarusti V, Boemel G, Dagnelie G, de Juan E Jr. Visual perception in a blind subject with a chronic microelectronic retinal prosthesis. Vision Res 2003;43:2573–2581
9. Laube T, Schanze T, Brockmann C, Bolle I, Stieglitz T, Bornfeld N. Chronically implanted epidural electrodes in Göttinger minipigs allow functional tests of epiretinal implants. Grafe's Arch Clin Exp Ophthalmol 2003;241:1013–1019
10. Walter P, Heimann K. Evoked cortical potentials after electrical stimulation of the inner retina in rabbits. Grafe's Arch Clin Exp Ophthalmol 2000;238:315–318
11. Kanda H, Morimoto T, Fujikado T, Tano Y, Fukuda Y, Sawai H. Electrophysiological studies of the feasibility of suprachoroidal-transretinal stimulation for artificial vision in normal and RCS rats. Invest Ophthalmol Vis Sci 2004;45:560–566
12. Nakauchi K, Fujikado T, Kanda H, Morimoto T, Choi JS, Ikuno Y, Sakaguchi S, Kamei M, Ohji M, Yagi T, Nishimura S, Sawai H, Fukuda Y, Tano Y. Transretinal electrical stimulation by an intrascleral multichannel electrode array in rabbit eyes. Grafe's Arch Clin Exp Ophthalmol 2005;243:169–174
13. Sieglitz T, Beutel H, Meyer JU. A flexible, light-weight multichannel sieve electrode with integrated cables for interfacing regenerating peripheral nerves. Sensors Actuators A 1997;60: 240–243
14. Rizzo JF III, Wyatt J, Lowenstein J, Kelly S, Shire D. Methods and perceptual thresholds for short-term electrical stimulation of human retina with microelectrode arrays. Invest Ophthalmol Vis Sci 2003;44;5355–5361
15. Brummer SB, Turner MJ. Electrical stimulation with Pt electrodes: II Estimation of maximum surface redox (theoretical non-gassing) limits. IEEE Trans Biomed Eng 1977;24:440–443
16. Tokuda T, Pan YL, Uehara A, Kagawa K, Nunoshita M, Ohta J. Flexible and extendible neural interface device based on cooperative multi-chip CMOS LSI architecture. Sensors Actuators A 2005;122:88–98
17. Licari JJ. Coating materials for electronic applications. New York: Noyes, 2003
18. Wolgemuth L. The surface modification properties of parylene for medical applications. Business Brief Med Device Manuf Technol 2002;1–4
19. Noh HS, Huang Y, Hesketh PJ. Parylene micromolding, a rapid and low-cost fabrication method for parylene microchannels. Sensors Actuators B 2004;102:78–85
20. Brummer SB, Turner MJ. Electrochemical considerations for safe electrical stimulation of the nervous system with platinum electrodes. IEEE Trans Biomed Eng 1977;24:59–63
21. Rose TL, Robblee LS. Electrical stimulation with Pt electrodes. VIII. Electrochemically safe charge injection limits with 0.2-ms pulses. IEEE Trans Biomed Eng 1990;37:1118–1120
22. Brummer SB, Turner MJ. Electrical stimulation with Pt electrodes: I A method for determination of "real" electrode areas. IEEE Trans Biomed Eng 1977;24:436–439
23. Kelliher EM, Rose TL. Evaluation of charge injection properties of thin film redox materials for use as neural stimulation. Mat Res Soc Symp Proc 1989;110:23–27
24. Cogan SF, Troyk PR, Ehrlich J, Plante TD. In vitro comparison of the charge-injection limits of activated iridium oxide (AIROF) and platinum-iridium microelectrodes. IEEE Trans Biomed Eng 2005; 52:1612–1614
25. Weiland JD, Anderson DJ, Humayun MS. In vitro electrical properties for iridium oxide versus titanium nitride stimulating electrodes. IEEE Trans Biomed Eng 2002;49:1574–1579
26. Beebe X, Rose TL. Charge injection limits of activated iridium oxide electrodes with 0.2-ms pulses in bicarbonate buffered saline. IEEE Trans Biomed Eng 1988;35:494–495
27. Janders M, Egert U, Stelze M, Nisch W. Novel thin-film titanium nitride microelectrodes with excellent charge transfer capability for cell stimulation and sensing applications. Proceedings of the 19th International Conference IEEE/EMBS. Piscataway: IEEE, 1996:1191–1193

(12)

Artificial Vision: Vision of a Newcomer

Takashi Fujikado[1], Hajime Sawai[2], and Yasuo Tano[3]

Department of Applied Visual Science[1], *Department of Physiology*[2], *and Department of Ophthalmology*[3], *Osaka University Medical School*

Correspondence to: Yasuo Tano, M.D.

Department of Ophthalmology, Osaka University Medical School

Rm E-7, 2-2 Yamadaoka, Suita, 565-0871, Japan